JCTC Journal of Chemical Theory and Computation

DFT Study and Monte Carlo Simulation on the Aminolysis of $XC(O)OCH_3$ (X = NH_2, H, and CF_3) with Monomeric and Dimeric Ammonias

Xuefei Xia,[†] Chenghua Zhang,[†] Ying Xue,*[,†,‡] Chan Kyung Kim,[§] and Guosen Yan[†]

College of Chemistry, Key Laboratory of Green Chemistry and Technology in Ministry of Education, Sichuan University, Chengdu 610064, P. R. China, State Key Laboratory of Biotherapy, Sichuan University, Chengdu 610041, P. R. China, and Department of Chemistry, Inha University, Inchon 402-751, Korea

Received March 24, 2008

Abstract: The aminolysis of substituted methylformates ($XC(O)OCH_3$, X = NH_2, H, and CF_3) in the gas phase and acetonitrile are investigated by the density functional theory B3LYP/6−311+G(d,p) method and Monte Carlo (MC) simulation with free energy perturbation (FEP) techniques. The direct and the ammonia-assisted aminolysis processes are considered, involving the monomeric and dimeric ammonia molecules, respectively. In each case, two different pathways, the concerted and stepwise, are explored. The calculated results show that, for the direct aminolysis, the activation barrier of the concerted path is lower than that of the rate-controlling step of the stepwise process for all three reaction systems. In contrast, for the ammonia-assisted mechanism, the stepwise process is more favorable than the concerted pathway. The substituent effects at the carboxyl C atom of methylformate are discussed. This aminolysis of substituted methylformates is more favored for X = CF_3 than for X = H and NH_2 in the gas phase for both the direct and the ammonia-assisted processes. Solvent effects of CH_3CN on the reaction of $HC(O)OCH_3 + nNH_3$ (n = 1, 2) are determined by Monte Carlo simulation. The potential energy profiles along the minimum energy paths in the gas phase and in acetonitrile are obtained. It is shown that CH_3CN lowers the energy barriers of all reactions.

1. Introduction

As the model for the formation of peptide bonds, the aminolysis of esters involved in the interaction of carbonyl group with nucleophile is under active investigation by using experimental and theoretical methods.[1−15] Up to now, three possible reaction pathways in accordance with the available kinetic results have been generally discussed in literature. The first one is the concerted pathway where the cleavage of C−O bond, the formation of C−N bond, and the transfer of H atom from the N atom at amine to the O atom proceed simultaneously. The second is the stepwise (addition/elimination) mechanism through neutral intermediates. The final way is the stepwise process involving zwitterionic intermediates in the reaction. Solvent effects of acetonitrile as well as the general base catalysis by the amine have been studied.[3,4]

Some authors made efforts to theoretically study the stepwise pathway through zwitterionic intermediates.[13−17] Gorb et al.[16] used three kinds of solvent models to study the mechanism of formamide hydrolysis from *ab initio* calculations and QM/MM molecular dynamics simulations. Their calculations showed that the zwitterionic intermediate is quite easily dissociated and could play a role in the hydrolysis of substituted amides or peptides. When Chalmet et al.[17] reported a theoretical study on the model reaction of ammonia and formic acid, their computations with the continuum model did not predict a stable zwitterionic intermediate, whereas a local energy minimum was found by explicit consideration of four solvent water molecules.

* Corresponding author e-mail: yxue@scu.edu.cn.

[†] Key Laboratory of Green Chemistry and Technology in Ministry of Education, Sichuan University.

[‡] State Key Laboratory of Biotherapy, Sichuan University.

[§] Inha University.

10.1021/ct800099a CCC: $40.75
Published on Web 09/04/2008

For the reaction of methylformate with ammonia, Ilieva et al. did not succeed in applying the MP2/6−31G(d, p) method to identify zwitterionic transition states and intermediates.[18] They reported that two explicit water molecules are needed to obtain a very shallow minimum. When concerning the formation of a zwitterion between methylformate and ammonia and hydrazine in water, Singleton and Merrigan[19] used the B3LYP/6−31G(d, p) method to calculate various solvated structures involving from four to eleven explicit water molecules; however, they failed to find global minima for these structures. Recently, Sung and his cooperators[20] have studied the structures and stability of zwitterionic complexes in the aminolysis of phenyl acetate with ammonia and pointed out that at least five explicit water molecules are needed to stabilize the zwitterionic intermediate.

Differences in the ester structures,[21−25] amine nature,[26−28] and reaction medium[21,29] can result in changes in the reaction mechanism and the rate determining step. Antonczak et al.[30] first examined electrostatic solvent effects on the hydrolysis of formamide by using a dielectric continuum solvent model. Besides, they particularly studied the water-assisted hydrolysis processes at the MP3/6−31G**//3−21G *ab initio* level. They suggested that electrostatic interactions with the continuum should not significantly modify the energetics of the process. Sordo et al.[31−38] thoroughly investigated the possible mechanisms of the aminolysis reaction systems, such as the aminolysis reaction between the ϵ-amino group of Lysine 199 and benzylpenicillin,[31] the water-assisted aminolysis of 2-azetidinone,[32,35] the aminolysis of monocyclic β-lactams,[33] the NH_3-assisted aminolysis of β-lactams[34] and penicillins,[37] and the aminolysis of monobactams.[38] When they studied the aminolysis of β-lactams, they predicted that positively charged ethanolamine molecules can act as bifunctional catalysts.[36] In addition, they also considered water-assisted mechanistic routes and the solvent effects. Ilieva and his co-workers[18] studied the aminolysis of methylformate with the QCISD/6−31G(d, p) and B3LYP/6−31G(d) methods and found that the neutral stepwise and the concerted pathways have very similar activation energy, and the presence of aprotic solvent acetonitrile fully lowers all energy barriers. For the aminolysis of 2-benzoxazolinone with methylamine, Ilieva et al.[39] predicted theoretically the concerted mechanism is most favorable in all three possible pathways at the B3LYP/6−31G(d) level of theory. Zipse et al.[12,13] studied the mechanism of the reaction of methyl acetate with methylamine and obtained the single point MP2/6−31G(d, p) energies through the HF/3−21G and HF/6−31G(d, p) optimized structures. Their results indicated that the stepwise (addition/elimination) pathway is more favorable than the concerted pathway. However, Jin et al.[40] found that the reaction prefers the concerted pathway to the neutral stepwise process in the gas phase and solutions concerning the aminolysis of phenylformate.

To our knowledge, few efforts have been made to investigate systemically the substituent effects on the ester aminolysis by applying a higher level of electron structure theory and solvent effects determined by Monte Carlo simulation from a theoretical point of view. We employed the density functional theory B3LYP/6−31G(d, p) method to study the substituent effects of the leaving groups on aminolysis of p-substituted phenyl acetates with ammonia.[41] In the present work, we aim to examine the effects of the nonleaving group substituents and solvents on the aminolysis of methylformates $XC(O)OCH_3$ (X = H, NH_2, and CF_3). In each case of the concerted and stepwise pathways, two processes, the direct aminolysis (with monomeric ammonia molecule) and the ammonia-assisted aminolysis (with dimeric ammonia), are considered (see Scheme 1). For the gas-phase reactions, the hybrid density functional theory (B3LYP) has been used in our calculations. In our previous work, we adopted the quantum chemical molecular orbital method and the Monte Carlo (MC) simulation with the free energy perturbation (FEP) technique to study the effects of solvents on the aza-Wittig reaction of iminophosphoranes,[42] the isomerization of imidazolines,[43] and the hydrolysis of N-(2-oxo-1,2-dihydropyrimidinyl) formamide.[44] In this study, the potential energy profiles of the direct and ammonia-assisted aminolysis processes of the compound methylformate in the gas phase and in CH_3CN are obtained. The effect of solvent CH_3CN is studied using the Monte Carlo free energy perturbation method.

2. Computational Details

2.1. Gas-Phase Calculation. All calculations were carried out using Gaussian 03 program package.[45] To test the reliability of the theoretical approaches for the calculation of the energetics of reaction systems, we performed calculations for the concerted process of the direct aminolysis of the $HC(O)OCH_3$ molecule with a variety of calculational levels such as HF/6−31G(d, p), B3LYP/6−31G(d, p), B3LYP/6−311+G(d, p), MP2/6−31G (d, p), MP2/6−311+G (d, p), and G2(MP2). Comparison of the results obtained by the methods above indicated that the B3LYP/6−311+G(d, p) level is acceptable and a relatively economical option in this work (see the detailed discussion in the next section). Therefore, the B3LYP/6−311+G(d, p) method was selected for the ensuing calculations on the title reactions.

The geometric structures of all the reactant complexes, product complexes, intermediates, and transition states of aminolysis of $XC(O)OCH_3$ (X = H, NH_2, and CF_3) reaction systems were optimized at the B3LYP/6−311+G(d, p) level. The harmonic vibrational frequencies of each stationary point were calculated at the same level by diagonalizing the force constant matrix to characterize it as a true minimum with no imaginary frequency or a transition state with only one imaginary frequency. The frequency calculations without scaling also provided the thermodynamic quantities such as the zero-point vibrational energy, thermal correction, enthalpies, Gibbs free energies, and entropies at a temperature of 298.15 K and a pressure of 1.0 atm.

All transition states were checked by intrinsic reaction coordinate (IRC)[46] calculations. In the IRC calculations for the $HC(O)OCH_3 + nNH_3$ (n = 1, 2) reaction systems, the "IRC=tight" option was used to generate the minimum energy path (MEP) in the gas phase. The MEPs at the B3LYP/6−311+G(d, p) level were constructed with a step size of 0.05 amu1/2 bohr. For all points along MEP, the

Scheme 1. Reaction Paths of the Aminolysis of $XC(O)OCH_3$ (X = NH_2, H, and CF_3) with Monomeric and Dimeric Ammonia Molecules

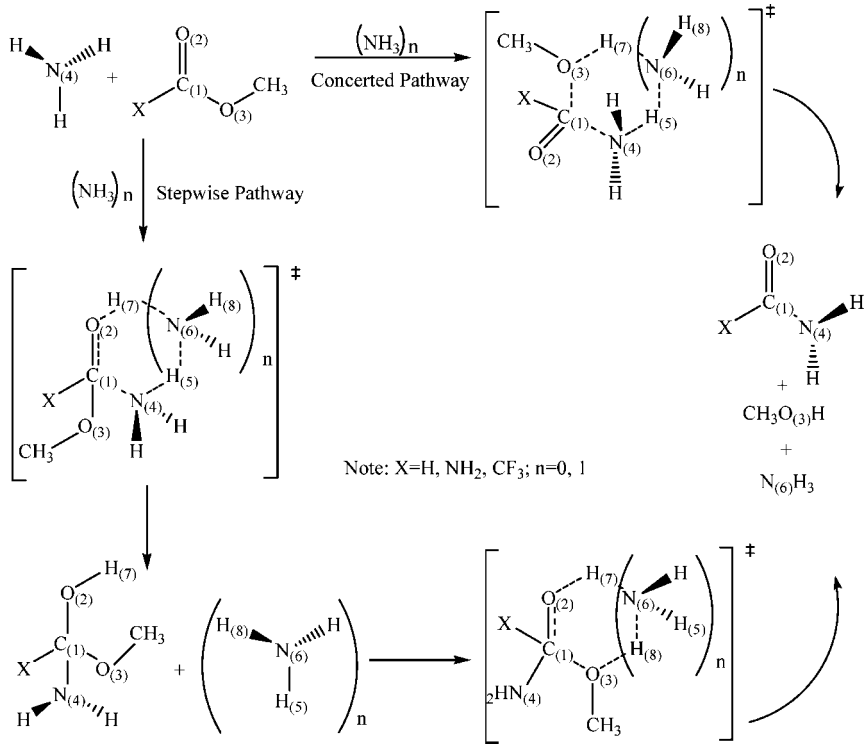

partial atomic charges were obtained via the Natural Bond Orbital Theory (NBO)[47] at the B3LYP/6−311+G(d, p) level.

2.2. Monte Carlo Simulation. CH_3CN was used as solvent to study the solvent effects on the aminolysis of methylformate by the Monte Carlo simulation with statistical perturbation theory.[48] Given a distance r_{ij} between atom i in molecule A and atom j in molecule B, the intermolecular interaction potential function for solute−solvent and solvent−solvent interactions was described by Coulomb and Lennard-Jones terms as shown in eq 1

$$\Delta E_{AB} = \sum\sum \{q_i q_j e^2/r_{ij} + 4\varepsilon_{ij}[(\sigma_{ij}/r_{ij})^{12} - (\sigma_{ij}/r_{ij})^6]\} \quad (1)$$

The crossing terms σ_{ij} and ε_{ij} in eq 1 were obtained by the combination rules

$$\sigma_{ij} = \sqrt{\sigma_{ii} \times \sigma_{jj}}, \quad \varepsilon_{ij} = \sqrt{\varepsilon_{ii} \times \varepsilon_{jj}} \quad (2)$$

No intramolecular terms were included. The ϵ and σ constants for the solute were taken from the OPLS all-atom parameters of the BOSS 4.2 database.[49] As the partial charge of atom i, the q_i was obtained from the gas-phase calculation above. For the solvent CH_3CN, the OPLS united-atom models were adopted, and the parameters were also taken from the BOSS 4.2 database.

For the reaction path obtained by DFT studies, the geometries and partial charges along the minimum energy path (MEP) were incorporated into a molecular mechanical potential presented by eq 1 for the reaction system and then applied to calculate free energy changes of solvation along the MEP. The reaction system was immersed in the periodic box containing 390 explicit solvent molecules, which had dimensions of 26.7 Å × 26.7 Å × 40.0 Å. Preferential sampling was applied in the Metropolis algorithm, and the perturbations were performed using double-wide sampling in 51, 95, 51, and 77 windows for the concerted mechanism in the direct aminolysis reaction (designated DC), the stepwise mechanism of the direct aminolysis reaction (DS), the ammonia-assisted aminolysis reaction through the concerted mechanism (AC), and the ammonia-assisted aminolysis reaction through the stepwise mechanism (AS) in solvent CH_3CN, respectively. Every simulation included 2×10^6 configurations for equilibration, followed by 4×10^6 configurations of averaging in the isothermal, isobaric (NPT) ensemble at 298.15 K and 1 atm. For the solute−solvent and solvent−solvent interactions, a cutoff of 12.0 Å was employed for solvent CH_3CN. Finally we added the gas-phase relative energies to the computed free energy changes of solvation for obtaining the total potential energy profile along the reaction path in solution. All Monte Carlo simulation calculations were performed using the BOSS 4.2 program package.[49]

3. Results and Discussions

3.1. Test Calculations. For an accurate estimation of the energies, the concerted process in the direct aminolysis of $HC(O)OCH_3$ was studied at different computational levels and basis sets up to G2(MP2). The thermodynamic data relative to the reactant complex are listed in Table 1. Because the experimental results on this step are unavailable, it is impossible to carry out the comparison between theoretical and observed activation barriers. However, the theoretically predicted activation data at the G2(MP2) level of theory can serve as benchmark values for comparison (see Table 1). One can see from Table 1 that the HF/6−31G(d, p) method overestimates the activation electronic energies, enthalpies,

Table 1. Activation Energies ($\Delta E^{\ddagger}$), Zero-Point Vibrational Energies ($\Delta E_{ZPV}{}^{\ddagger}$), Enthalpies ($\Delta H^{\ddagger}$), and Gibbs Free Energies ($\Delta G^{\ddagger}$) in the Concerted Pathway of Aminolysis of $HC(O)OCH_3$ at Different Levels of Theory[a]

methods	$\Delta E^{\ddagger}$	$\Delta E_{zpv}{}^{\ddagger}$	$\Delta H^{\ddagger}$	$\Delta G^{\ddagger}$
HF/6−31G(d, p)	66.89	65.61	64.20	67.96
B3LYP/6−31G(d, p)	44.03	42.45	41.05	44.82
B3LYP/6−311+G(d, p)	44.96	43.59	42.11	46.35
MP2/6−31G(d, p)	46.26	44.63	43.22	46.92
MP2/6−311+G(d, p)	45.66	44.25	42.75	46.95
G2(MP2)		46.47	45.11	48.90

[a] In kcal/mol.

and Gibbs free energies in comparison with the G2(MP2) values and is poor in describing the aminolysis reactions of methylformate. The best agreement with those reference values comes from $\Delta E_{zpv}{}^{\ddagger}$, $\Delta H^{\ddagger}$, and $\Delta G^{\ddagger}$ values determined at the MP2/6−31G(d, p) level, the computed differences being less than 2.0 kcal/mol. The use of the larger basis set 6−311+G(d, p) in the MP2 approach slightly decreases the activation electronic energy and enthalpy. The results performed at the B3LYP level are quite close to those derived from the MP2 method, and the largest difference of 2.23 kcal/mol appears for the activation electronic energy $\Delta E^{\ddagger}$. The enlarging of the basis set from 6−31G(d, p) to 6−311+G(d, p) improves a bit of the performance of the B3LYP functional. The computed energy barrier with zero-point vibrational energy correction for this concerted step amounts to 43.59 and 46.47 kcal/mol at the B3LYP/6−311+G(d, p) and the G2(MP2) levels of theory, respectively. The corresponding Gibbs free energy changes are also similar, 46.35 kcal/mol for B3LYP/6−311+G(d, p) and 48.90 kcal/mol for G2(MP2), respectively. Therefore, it can be concluded that the B3LYP/6−311+G(d, p) level is suitable to study the title reaction with a good compromise between accuracy and computational cost.

3.2. Structures of Stationary Points in the Gas Phase. Here the concerted and stepwise pathways in each of the direct and ammonia-assisted mechanisms were considered for the aminolysis of the parent methylformate, similar to the cases in the previous theoretical study.[18] The calculated results show that these two cases are different in the attack manner, and the proton transfer is the main factor that influences the energy barrier. When the hydrogen atom H at the carbonyl C atom in methylformate was replaced by the NH_2 or CF_3 group, it was observed that the mechanism and all the critical structures of the reaction systems are similar to those when X = H for either concerted or neutral stepwise pathways. The main optimized geometrical parameters of all transition states along the reaction paths are given in Figure 1 for the reactions of $XC(O)OCH_3$ (X = NH_2, H, and CF_3) with the monomeric and dimeric ammonia molecules.

For the concerted pathway of the direct aminolysis of methylformate, the reaction involves only one step, in which the creation of the $C_{(1)}$-$N_{(4)}$ bond, the destruction of the $C_{(1)}$-$O_{(3)}$ bond, and the proton $H_{(5)}$ transfer from the ammonia toward $O_{(3)}$ occur in concert. The nucleophilic ammonia molecule attaches to the electrophilic carbon atom $C_{(1)}$, and a proton $H_{(5)}$ transfer from the ammonia molecule toward

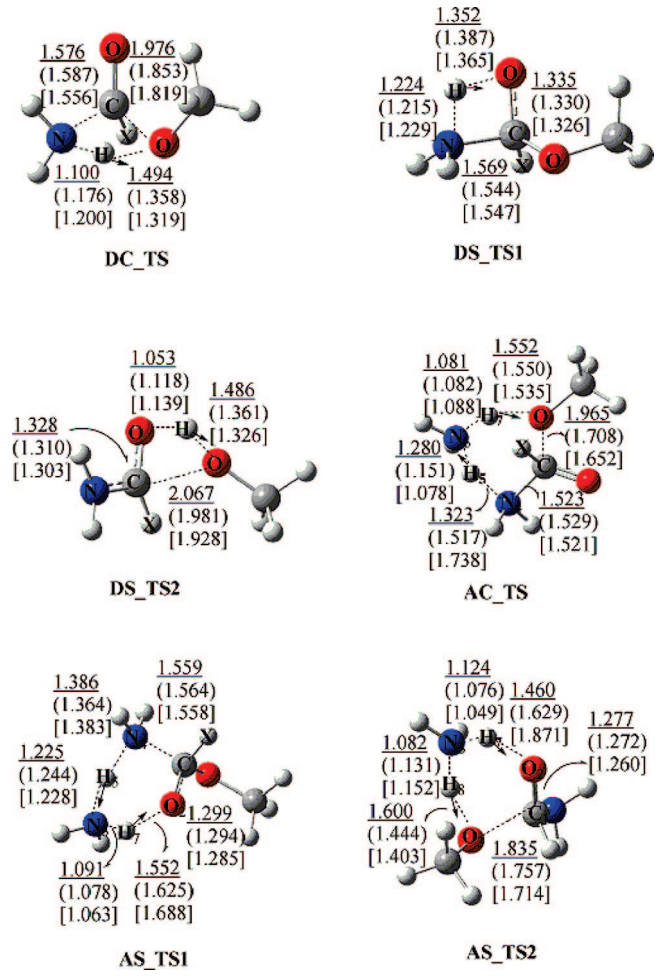

Figure 1. Optimized transition structures along the concerted and stepwise pathways for the aminolysis of $XC(O)OCH_3$, (X = NH_2 (underlined), H (in parentheses), and CF_3 (in square brackets)). The arrows on the transition states indicate the reaction coordinate. (Bond lengths are in Å.)

the ester oxygen atom $O_{(3)}$ simultaneously occurs. The transition state (designated DC_TS) has a four-membered ring structure constituted by $C_{(1)}$, $O_{(3)}$, $H_{(5)}$, and $N_{(4)}$ atoms. IRC calculations in the reverse and forward directions from the transition state cause producing of the reactant complex (DC_RC) and the product complex (DC_PC). The stepwise pathway for the direct aminolysis of methylformate is mainly an addition/elimination mechanism. For both addition and elimination steps, proton transfers are involved to maintain neutrality in the tetrahedral intermediates formed. Calculated results showed this reaction begins with the addition of the $N_{(4)}$-$H_{(5)}$ bond to the $C_{(1)}$=$O_{(2)}$ double bond and consists of two transition states. The first transition state DS_TS1 has a four-membered ring consisting of $C_{(1)}$, $O_{(2)}$, $H_{(5)}$, and $N_{(4)}$ atoms and involves proton $H_{(5)}$ transfer from $N_{(4)}$ toward the carbonyl oxygen atom $O_{(2)}$. IRC calculations from the forward direction indicated that DS_TS1 converts to the stable intermediate DS_INT, in which the $C_{(1)}$-$N_{(4)}$ bond is formed, and proton $H_{(5)}$ is already transferred to $O_{(2)}$. The second step of the process is an elimination reaction, in which the $C_{(1)}$-$O_{(3)}$ ester single bond is broken, proton H_5 transfers from $O_{(2)}$ to $O_{(3)}$, and at the same time the $C_{(1)}$=$O_{(2)}$ bond is

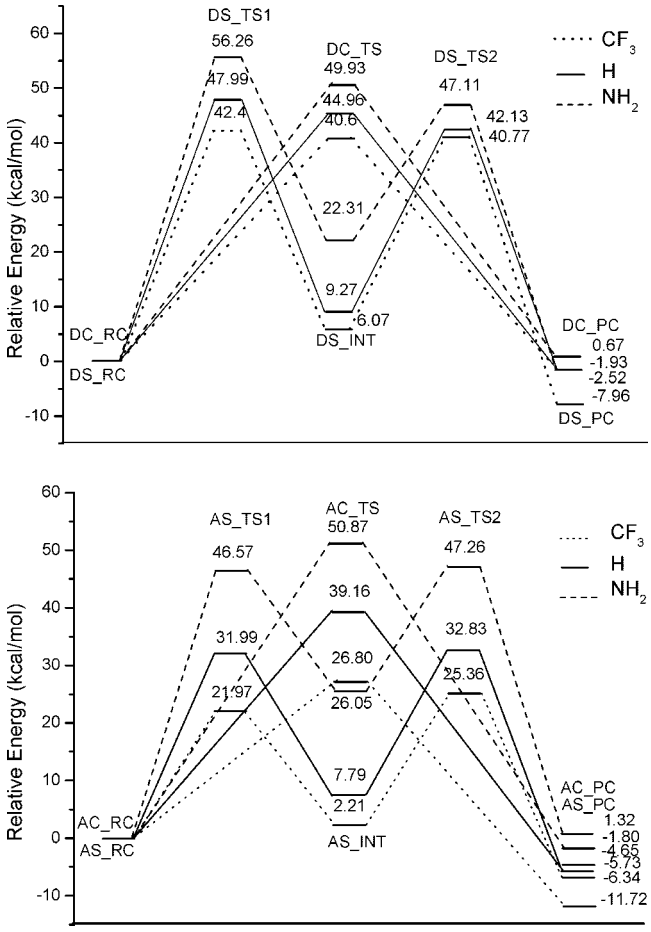

Figure 2. Potential energy profiles for the aminolysis of different substituted methylformates along the concerted and stepwise mechanisms in the gas phase.

simultaneously restored. The transition state DS_TS2 also has a four-membered ring including $C_{(1)}$, $O_{(3)}$, $H_{(5)}$, and $O_{(2)}$ atoms.

The ammonia-assisted aminolysis reaction involves two ammonia molecules: the first ammonia molecule could be considered as the nucleophilic agent, while the second ammonia molecule acts as a catalytic role of facilitating the proton transfer. We also considered two mechanisms: the concerted and the stepwise pathways for this ammonia-assisted reaction of methylformate. From Figure 1, in the concerted process, the transition state AC_TS involves the simultaneous creation of the $C_{(1)}$-$N_{(4)}$ bond, the destruction of the $C_{(1)}$-$O_{(3)}$ bond, and the proton $H_{(5)}$ from ammonia as the nucleophilic agent toward the assisted-ammonia and the other proton $H_{(7)}$ transfer from the assisted-ammonia toward $O_{(3)}$. Similarly, the stepwise case in the ammonia-assisted reaction is coupled with proton transfer to keep neutrality in the hexahedral intermediates formed. As can be seen from Figure 1, the first transition state AS_TS1 contains a six-membered cycle constituted by $C_{(1)}$, $O_{(2)}$, $H_{(5)}$, $N_{(4)}$, $H_{(7)}$, and $N_{(6)}$ atoms and involves the proton $H_{(7)}$ transfer from $N_{(6)}$ toward the carbonyl $O_{(2)}$ and the other proton $H_{(5)}$ from ammonia as the nucleophilic reagent toward the assistant ammonia. Overcoming AS_TS1, the stable intermediate AS_INT is obtained, in which the $C_{(1)}$-$N_{(4)}$ bond is formed and the proton $H_{(7)}$ is already transferred to form a hydroxyl group. The second step of the process is similar to that of DS, associated with the breaking of the $C_{(1)}$-$O_{(3)}$ ester single bond and the simultaneous restoration of the $C_{(1)}$=$O_{(2)}$ bond after proton transfer. In the process of proton transfer, the transfer of $H_{(7)}$ from the hydroxyl group to the assistant ammonia and the transfer of another proton $H_{(8)}$ from the assistant ammonia to $O_{(3)}$ proceed in concert, in which the assistant ammonia acts as a role of proton-transfer catalysis. Compared with Sonia Ilieva's related work on the aminolysis of methylformate,[18] we adjusted the orientations of reaction complexes and transition states and located only one intermediate between AS_TS1 and AS_TS2.

3.3. Energetics. The computed relative electronic energies (ΔE), corrected zero-point vibrational energies (ΔE_{ZPV}), enthalpies (ΔH), and Gibbs free energies (ΔG) (relative to the reactant complex) for the fully optimized structures along the DC, DS, AC, and AS processes of aminolysis of $XC(O)OCH_3$ (X = NH_2, H, and CF_3) are given in the Supporting Information. The potential energy profiles are presented in Figure 2. The thermodynamic data were calculated using the B3LYP/6−311+G(d, p) method at 298.15 K and 1 atm.

In the direct aminolysis reaction, for the concerted pathway (DC), the activation energies increase in the following order: CF_3 (40.60 kcal/mol) < H (44.96 kcal/mol) < NH_2 (49.93 kcal/mol); while for DS, the activation energy changes agree with the order CF_3 (42.40 kcal/mol) < H (47.99 kcal/mol) < NH_2 (56.26 kcal/mol) for the addition step, and CF_3 (40.77 kcal/mol) < H (42.13 kcal/mol) < NH_2 (47.11 kcal/mol) for the elimination step, respectively. So the rate-determining step of the stepwise process is the addition reaction. Compared with the concerted mechanism, the activation energies of the stepwise mechanism are 6.33, 3.03, and 1.80 kcal/mol higher for X = NH_2, H, and CF_3, respectively. With regard to the parent compound, the electron-withdrawing group CF_3 lowers the energy barriers by 4.36 and 5.59 kcal/mol for the concerted and stepwise mechanism, respectively, whereas the electron-donating NH_2 group increases the energy barriers by 4.97 and 8.27 kcal/mol. It can be seen that B3LYP/6−311+G(d, p) calculations in the gas phase predict the concerted mechanism for all three aminolysis reactions to be more favorable than the stepwise pathway. These theoretical findings are in qualitative accord with the findings of Ilieva for the aminolysis of methylformate[18] and Yang and Drueckhammer for the aminolysis of methylthionacetate.[14] Latter authors showed that the gas-phase energies of the transition states for stepwise and concerted pathways are very close. More definite conclusions for the preferred mechanism may be made if the general base-catalyzed aminolysis process is considered.

In the ammonia-assisted aminolysis reaction, for the AC path, the activation energies increase in the following order: CF_3 (26.80 kcal/mol) < H (39.16 kcal/mol) < NH_2 (50.87 kcal/mol); while for AS, the activation energy changes agree with the order CF_3 (21.97 kcal/mol) < H (31.99 kcal/mol) < NH_2 (46.57 kcal/mol) for the addition step, and CF_3 (25.36 kcal/mol) < H (32.83 kcal/mol) < NH_2 (47.26 kcal/mol) for the elimination step, respectively. So the rate-determining step of the stepwise process is the elimination reaction.

Table 2. Natural Charges (q) and Changes in Charges (Δq) for the Concerted and the Stepwise Pathways of the Aminolysis of Methylformate at the B3LYP/6-311+G(d, p) Level of Theory[a]

	Direct Aminolysis				
	C_1	O_2	N_4	H_5	O_3
q^{DC_RC}	0.650	−0.612	−1.069	0.349	−0.537
Δq^{DC_TS}	−0.087	−0.036	0.208	0.125	−0.216
Δq^{DC_PC}	−0.128	−0.011	0.248	0.119	−0.214
q^{DS_RC}	0.649	−0.612	−1.069	0.370	−5.373
Δq^{DS_TS1}	−0.057	−0.224	0.232	0.105	4.730
Δq^{DS_INT}	−0.077	−0.131	0.201	0.100	4.761
q^{DS_INT}	0.572	−0.743	−0.868	0.469	−0.612
Δq^{DS_TS2}	0	−0.001	0.110	0.041	−0.175
Δq^{DS_PC}	−0.042	0.107	0.073	0.013	−0.157

	Ammonia-Assisted Aminolysis							
	C_1	O_3	N_4	H_5	H_7	N_6	O_2	H_8
q^{AC_RC}	0.636	−0.575	−1.089	0.391	0.377	−1.080	−0.588	0.355
Δq^{AC_TS}	−0.055	−0.209	0.175	0.051	0.091	0.112	−0.155	0.037
Δq^{AC_PC}	−0.122	−0.224	0.288	0.011	0.121	−0.010	−0.067	0.004
q^{AS_RC}	0.644	−0.540	−1.092	0.394	0.388	−1.086	−0.629	0.353
Δq^{AS_TS1}	−0.055	−0.129	0.222	0.040	0.065	0.076	−0.233	0.035
Δq^{AS_INT}	−0.066	−0.080	0.213	−0.004	0.113	0.004	−0.145	0.010
q^{AS_INT}	0.578	−0.620	−0.879	0.390	0.500	−1.082	−0.773	0.363
Δq^{AS_TS2}	−0.011	−0.122	−0.016	0.012	−0.046	0.131	−0.033	0.098
Δq^{AS_PC}	−0.058	−0.184	0.056	−0.022	−0.130	0.016	0.141	0.140

[a] In electronic charge units.

Table 3. Activation Energies ($\Delta E^{\ddagger}$), Reaction Energies (ΔE^{o}), Intrinsic Barrier ($\Delta E_o^{\ddagger}$), and Thermodynamic Contributions ($\Delta E_{thermo}^{\ddagger}$) as well as Relative Values (in Parentheses) to the Parent Compound for the Concerted Pathway and the Addition/Elimination Steps of the Stepwise Pathway[a]

		X	$\Delta E^{\ddagger}$	ΔE^{o}	$\Delta E_o^{\ddagger}$	$\Delta E_{thermo}^{\ddagger}$
			Direct Aminolysis Reaction			
concerted		NH_2	49.93(4.97)	0.67(2.33)	49.59(3.80)	0.34(1.17)
		H	44.96(0.00)	−1.66(0.00)	45.79(0.00)	−0.83(0.00)
		CF_3	40.60(−4.36)	−1.42(0.24)	41.31(−4.48)	−0.71(0.12)
stepwise	I[b]	NH_2	56.26(8.27)	22.31(13.04)	44.40(1.17)	11.86(7.10)
		H	47.99(0.00)	9.27(0.00)	43.23(0.00)	4.76(0.00)
		CF_3	42.40(−5.59)	6.07(−3.20)	39.31(−3.92)	3.09(−1.67)
	II[c]	NH_2	24.80(−8.06)	−24.83(−13.63)	36.15(−2.11)	−11.35(−5.95)
		H	32.86(0.00)	−11.2(0.00)	38.26(0.00)	−5.40(0.00)
		CF_3	34.70(1.84)	−14.03(−2.83)	41.42(3.16)	−6.72(−1.32)
			Ammonia-Assisted Aminolysis Reaction			
concerted		NH_2	50.87(11.71)	−1.80(3.93)	51.77(9.79)	−0.90(1.92)
		H	39.16(0.00)	−5.73(0.00)	41.98(0.00)	−2.82(0.00)
		CF_3	26.80(−12.36)	−11.72(−5.99)	32.39(−9.59)	−5.59(−2.77)
stepwise	I[b]	NH_2	46.57(14.58)	26.05(18.26)	32.23(4.27)	14.34(10.31)
		H	31.99(0.00)	7.79(0.00)	27.96(0.00)	4.03(0.00)
		CF_3	21.97(−10.02)	2.21(−5.58)	20.85(−7.11)	1.12(−2.91)
	II[c]	NH_2	21.21(−3.83)	−24.73(−12.29)	32.40(1.45)	−11.19(−5.28)
		H	25.04(0.00)	−12.44(0.00)	30.95(0.00)	−5.91(0.00)
		CF_3	23.15(−1.89)	−8.55(3.89)	27.26(−3.69)	−4.11(1.80)

[a] In kcal/mol. [b] Addition step. [c] Elimination step.

Compared with the concerted mechanism, the activation energies of the stepwise mechanism are 3.61, 6.33, and 1.44 kcal/mol lower for X = NH_2, H, and CF_3, respectively. With regard to the parent compound, the electron-withdrawing group CF_3 substantially lowers the energy barriers by 12.36 and 7.47 kcal/mol for the concerted and stepwise mechanism, respectively, whereas the electron-donating NH_2 group increases the energy barriers by 11.71 and 14.43 kcal/mol. It can be seen that B3LYP/6−311+G(d, p) calculations in the gas phase for the ammonia-assisted aminolysis reaction predict the stepwise mechanism to be more favorable than the concerted pathway. In the structure AS_TS2, the second ammonia acting as the catalysis role facilities the proton-transfer between $O_{(2)}$ and $O_{(3)}$ and accordingly greatly lowers the activation energy. Compared with the concerted pathway of the direct aminolysis reaction, the stepwise progress of the ammonia-assisted aminolysis is 2.67, 12.13, and 15.24 kcal/mol more favored pathway for X = NH_2, H, and CF_3, respectively.

The atomic and group charges and their changes by the NBO method for the concerted pathway and addition/elimination steps of the stepwise pathway in the aminolysis of methylformate are shown in Table 2. For the direct aminolysis reaction, the DC_RC and DS_RC have positive

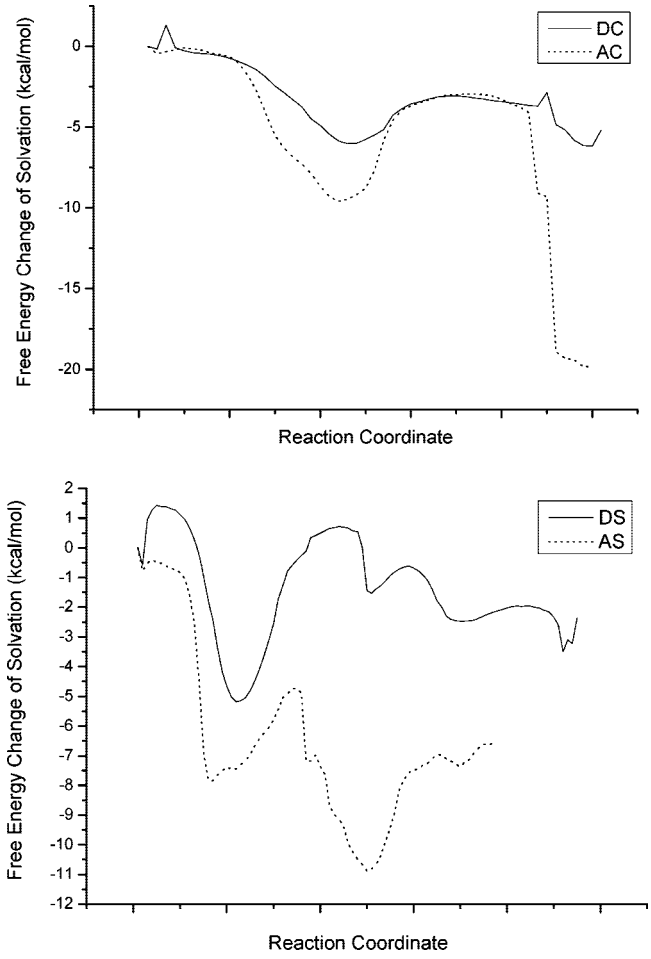

Figure 3. Changes in the free energies of solvation along the reaction coordinate calculated from Monte Carlo simulations.

charges on the $C_{(1)}$ group and negative charges on the $O_{(3)}$ group. In DC_TS and DS_TS1, the positive charges on the $C_{(1)}$ group decrease, while for the $O_{(3)}$ group, it becomes more negative in DC_TS and DS_TS1, suggesting that the rate should increase when the electron-withdrawing group CF_3 is the substituent. Therefore, the group CF_3 facilitates the reaction and is much more favorable for the aminolysis reaction. Accordingly, we can get the same conclusion when analyzing the ammonia-assisted aminolysis reaction.

3.4. Substituent Effects. To analyze the substituent effects on the activation energies of the aminlysis reaction, it is necessary to understand how substituents alter the energies. One useful way is to use the Marcus theory,[50] which was used to analyze the activation energies of reaction pathways.[51] The Marcus equation is given by

$$\Delta G^{\ddagger} = \Delta G_o^{\ddagger} + {}^1\!/_2\Delta G^{\circ} + (\Delta G^{\circ})^2/(16\Delta G_o^{\ddagger}) \qquad (3)$$

where $\Delta G_o^{\ddagger}$ is called the intrinsic barrier representing the barrier of a thermoneutral reaction. $\Delta G^{\ddagger}$ and ΔG° are Gibbs free energy changes of activation and reaction of a nondegenerate reaction, respectively. The third term $(\Delta G^{\circ})^2/(16\Delta G_o^{\ddagger})$ is the correction factor for nonadditivity of the intrinsic and thermodynamic effects. Murdoch advocated that the similar expression in eq 4 can be applied to the nondegenerate reaction and used for some pericyclic reactions and other chemical processes[52,53]

$$\Delta E^{\ddagger} = \Delta E_o^{\ddagger} + {}^1\!/_2\Delta E^{\circ} + (\Delta E^{\circ})^2/(16\Delta E_o^{\ddagger}) \qquad (4)$$

Table 4. Changes in the Free Energies of Solvation (ΔG_{sol}) and Total Free Energy Differences (ΔG_{total}) in the Gas Phase and the Solvent CH_3CN for DC, DS, AC, and AS Pathways of Aminolysis of Methylformate[a]

			gas phase	CH_3CN
DC		$\Delta G_{sol}^{\ddagger}$	–	−5.50
		$\Delta G_{total}^{\ddagger}$	46.35	40.85
		ΔG_{sol}^{o}	–	−5.19
		ΔG_{total}^{o}	−2.29	−7.48
DS	I[b]	$\Delta G_{sol}^{\ddagger}$	–	−3.12
		$\Delta G_{total}^{\ddagger}$	50.37	47.25
		ΔG_{sol}^{o}	–	0.02
		ΔG_{total}^{o}	14.91	14.93
	II[c]	$\Delta G_{sol}^{\ddagger}$	–	−2.45
		$\Delta G_{total}^{\ddagger}$	42.76	40.31
		ΔG_{sol}^{o}	–	−2.37
		ΔG_{total}^{o}	−2.84	−5.21
AC		$\Delta G_{sol}^{\ddagger}$	–	−9.19
		$\Delta G_{total}^{\ddagger}$	42.72	33.53
		ΔG_{sol}^{o}	–	−19.84
		ΔG_{total}^{o}	−5.01	−24.85
AS	I[b]	$\Delta G_{sol}^{\ddagger}$	–	−7.44
		$\Delta G_{total}^{\ddagger}$	35.90	28.46
		ΔG_{sol}^{o}	–	−7.16
		ΔG_{total}^{o}	13.42	6.26
	II[c]	$\Delta G_{sol}^{\ddagger}$	–	−9.43
		$\Delta G_{total}^{\ddagger}$	36.86	27.43
		ΔG_{sol}^{o}	–	−6.60
		ΔG_{total}^{o}	−6.67	−13.27

[a] In kcal/mol. [b] Addition step. [c] Elimination step.

In this study, we used eq 4 to separate the intrinsic and thermodynamic contributions of the substituent effects on the activation energies of the aminolysis of $XC(O)OCH_3$ reactions for the concerted mechanism and addition/elimination processes in the stepwise pathway. The intrinsic barrier $\Delta E_o^{\ddagger}$ was calculated using eq 4 with the quantum mechanically calculated values of activation energy $\Delta E^{\ddagger}$ and reaction energy ΔE°. Table 3 shows the intrinsic barriers and the thermodynamic contributions for the title reaction systems. For the direct aminolysis reaction, the intrinsic activation energies of the concerted mechanism and the addition step of the stepwise pathway of the parent system are 44.96, 47.99, and 32.86 kcal/mol, respectively. For the concerted mechanism, when X = CF_3, the 4.36 kcal/mol decrease in the activation is mainly due to the intrinsic factor, which induces a 4.48 kcal/mol decrease, and with only a 0.12 kcal/mol increase in exothermicity by the group. When X = NH_2, the relative high contributions of intrinsic (3.80 kcal/mol) and thermodynamic (1.17 kcal/mol) lead to a small increase in the activation energy. For the addition/elimination steps of the stepwise pathway, the intrinsic contribution is also a dominate factor in the activation energy reductions in the X = CF_3 reaction system, while for X = NH_2, the relative high contribution of the thermodynamic (7.10 kcal/mol) and the minor contribution of intrinsic (1.17 kcal/mol) lead to a considerable increase in the activation energy. For the ammonia-assisted aminolysis reaction, the intrinsic activation energies of the concerted mechanism and the addition/elimination steps of the stepwise pathway of the parent system are 39.16, 31.99, and 25.04 kcal/mol, respectively.

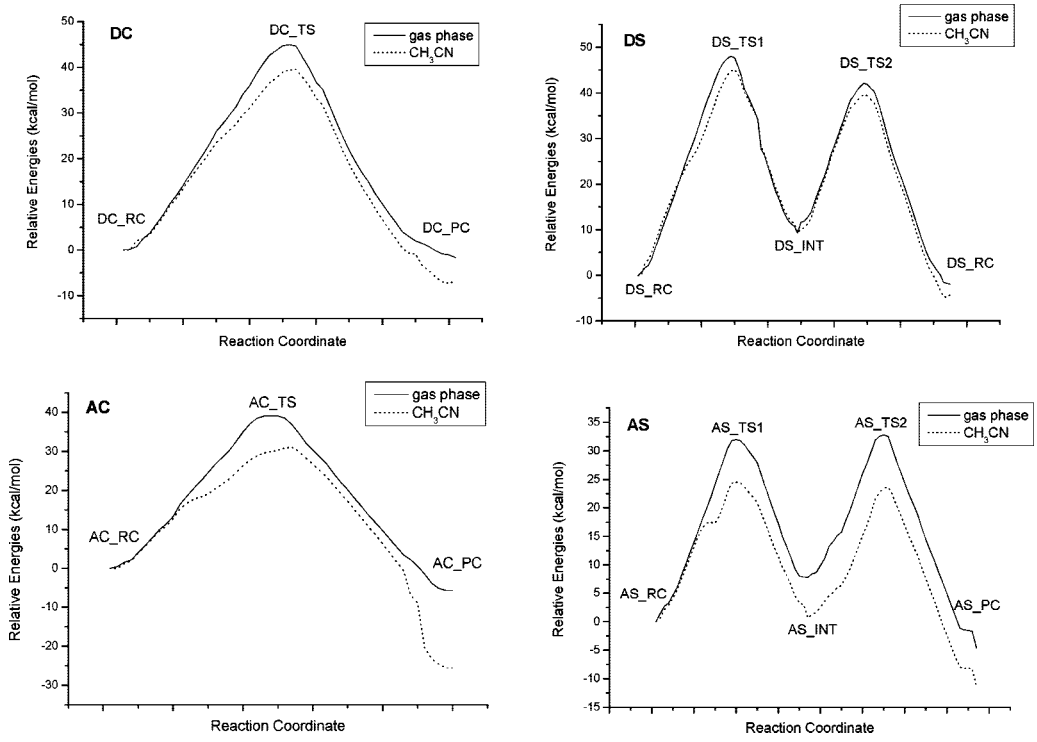

Figure 4. Minimum energy path $E_{MEP(s)}$ for the aminolysis of $HC(O)OCH_3$ in the gas phase and in the solvent CH_3CN.

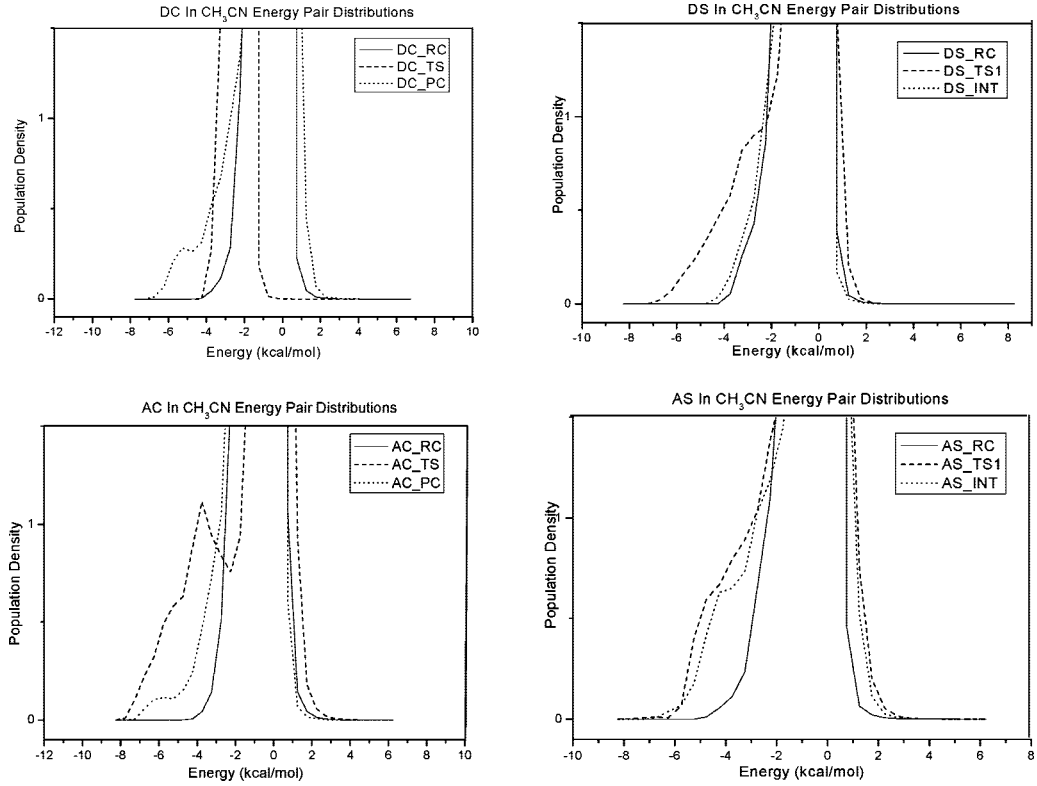

Figure 5. Energy pair distribution of solute−solvent interaction. The ordinate gives the number of solvent molecules coordinated with the solute with the interaction energy shown on the abscissa. The units for the *y*-axis are the number of molecules per kilocalorie per mole.

For the concerted mechanism, when $X = CF_3$, the 12.36 kcal/mol decrease in the activation is mainly due to the intrinsic factor, which induces a 9.59 kcal/mol decrease, and with only a 2.77 kcal/mol increase in exothermicity by the group. When $X = NH_2$, the relative high contributions of intrinsic (9.79 kcal/mol) and thermodynamic (1.92 kcal/mol) lead to a 11.71 kcal/mol increase in the activation energy. For the elimination step of the stepwise pathway, the intrinsic contribution is also a dominate factor in the activation energy reductions in the $X = CF_3$ reaction system, while for $X =$

NH_2, the relative high contribution of thermodynamic (−5.28 kcal/mol) and minor contribution of intrinsic (1.45 kcal/mol) lead to a decrease in the activation energy but with a high activation energy of 14.58 kcal/mol for the addition step of the stepwise pathway.

3.5. Solvent Effects Determined by Monte Carlo Simulation. The aminolysis of methylformate was studied in CH_3CN using the free energy perturbation method implemented in BOSS 4.2. The theoretical results confirm the conclusion made on the basis of calculations for the gas-phase process. Figure 3 displays the changes in free energies of solvation over the course of the reaction in the solvent CH_3CN. The changes in the free energies of solvation and free energy changes in the gas phase and in solution for the activation and DC, DS, AC, and AS reaction procedures are listed in Table 4. For DC, the difference in free energies of solvation between DC_RC and DC_TS in CH_3CN is −5.50 kcal/mol, which indicates that the transition state DC_TS is stabilized in CH_3CN by solvation compared with DC_RC. While for DS, the transition state DS_TS1 is stabilized more by solvation than the reactant complex DS_RC in CH_3CN and has 6.36 kcal/mol smaller free energies of solvation than DS_RC. It can be viewed from Table 4 that free energies of solvation of ammonia-assisted aminolysis reactions are considerably higher than those of the direct aminolysis reactions. For the solution, the calculated free energies of activation of the direct aminolysis by combining the DFT calculation (B3LYP/6−311+G(d, p) level) with the Monte Carlo simulation are 40.85, 47.25, 33.53, and 28.46 kcal/mol for DC, DS, AC, and AS in solvent CH_3CN. Figure 4 depicts the relative potential energy profiles $E_{MEP(s)}$ of four systems along the minimum energy path (MEP) in the gas phase and CH_3CN. From Table 4 and Figure 4, the solvent effects on the ammonia-assisted aminolysis of the concerted and stepwise pathways by CH_3CN are computed to be more favorable than those on the direct aminolysis of the two pathways. Thus, the calculations predict that a stepwise pathway with a NH_3 molecule as a catalyst in the solution is the preferred mechanism. Here comes a question: what factors are responsible for the solvent effects of CH_3CN. We consider the development of the electronic charge distribution on going from the reactant complex to the transition state. From Table 2, taking the direct aminolysis as an example, the reactant complex has a positive charge on atoms $C_{(1)}$ and $H_{(5)}$ and a negative charge on atoms $O_{(2)}$, $N_{(4)}$, and $O_{(3)}$. On going to the transition state DC_TS, when atoms $C_{(1)}$ and $H_{(5)}$ have net gains of electrons, atoms $O_{(2)}$, $N_{(4)}$, and $O_{(3)}$ have net losses of electrons. As a result, from DC_RC to DC_TS, the magnitude of charge on each of the atoms involved in the reaction center reduces, and the electronic charge distribution becomes more disperse, thus decreasing the electrostatic interaction with solvents. In contrast, for the ammonia-assisted process, there are net losses of electrons on atoms $C_{(1)}$ and $H_{(7)}$ and net gains of electrons on atoms $N_{(4)}$. On going from DS_RC to DS_TS1, the charges on atoms $C_{(1)}$ and $H_{(5)}$ become more positive, and the charges on atom $N_{(4)}$ become more negative. Such buildup of the electronic charges enhances the electrostatic interaction with solvents. The same conclusion has also been found in the stepwise pathway of both the direct transfer and ammonia-assisted aminolysis reactions.

Figure 5 shows the solute−solvent energy pair distributions for the DC, DS, AC, and AS processes. The plots give the number of solvent molecules on the ordinate that interact with the solute with the interaction energy shown on the abscissa. In the solution, the spikes centered at 0.0 kcal/mol result from the weak interactions between the solute and many distant CH_3CN molecules. In DC, from Figure 5(DC), for DC_RC in CH_3CN, there is a bound group of solvent molecules, which forms a band from ca. −10.0 to −2.25 kcal/mol. Integration of the distribution curve for DC_RC up to the end of this band at −2.25 kcal/mol defines 1.557 solvent molecules that interact with CH_3CN. Integration of the curves for DC_TS and DC_PC until this limit results in 10.433 and 4.657 CH_3CN molecules. In DS [see Figure 5(DS)], integration of the curves for DS_RC, DS_TS1, and DS_INT up to the end of this band at −2.25 kcal/mol defines 1.603, 4.532, and 2.185 CH_3CN molecules. In the AC system, integration of the curves up to the end of the plateaus at −2.25 kcal/mol reveals 2.333, 6.898, and 5.149 CH_3CN molecules for AC_RC, AC_TS, and AC_PC in CH_3CN, as shown in Figure 5(AC). For the AS system [see Figure 5(AS)], the number of CH_3CN molecules that interact with solute is 2.181, 5.878, and 4.950 for AS_RC, AS_TS1, and AS_INT. These differences imply that the stabilization of the transition structure relative to its reactant complex is different due to the effect of CH_3CN. The better solvation of the translate state in the ammonia-assisted path can be attributed to an increase in the interaction between solute and solvent molecules, while in the direct aminolysis process the decrease for the interactions with the solvent along the reaction path is responsible for the destabilization of translate state. The catalytic role of the second ammonia molecule affects mostly the proton-transfer processes. Thus six-member rings formed in the transition state structures for the catalyzed processes are more stable than four-member rings in the case of the uncatalyzed aminolysis reactions. This explains the lower energy barriers along the reaction path of the catalyzed process in the gas phase as well as in the presence of solvent CH_3CN.

4. Conclusion

The aminolysis of $XC(O)OCH_3$ (X = H, NH_2, and CF_3) was studied using the B3LYP/6−311+G(d, p) level of theory in the gas phase. The solvent effects of CH_3CN on the aminolysis of $HC(O)OCH_3$ were calculated by Monte Carlo simulations. The NH_3 catalysis role of the nucleophilic was investigated in detail. The results show that the most favorable pathway of the reaction is through the general base catalyzed neutral stepwise mechanism. The structure and transition vectors of the transition states indicate that the catalytic role of ammonia is realized by facilitating the proton transfer processes. The calculated values correctly reflect that the effect of CH_3CN is more favorable for the ammonia-assisted aminolysis than for the direct aminolysis. The calculated results indicate that the ammonia-assisted pathway is energetically preferred to the direct process in the gas

phase, and the electron-drawing group CF_3 facilitates all the aminolysis reaction processes.

Acknowledgment. This project has been supported by the National Natural Science Foundation of China (Grant Nos. 20473055 and 20773089) and the Scientific Research Foundation for the Returned Overseas Chinese Scholars, State Education Ministry (Grant No. 20071108-18-15).

Supporting Information Available: Listings of Cartesian coordinates and energies in hartrees at the B3LYP/6−311+G(d, p) level of theory. This material is available free of charge via the Internet at http://pubs.acs.org.

References

(1) Blackburn, G. M.; Jencks, W. P. The mechanism of the aminolysis of methyl formate. *J. Am. Chem. Soc.* **1968**, *90*, 2638.

(2) Jencks, W. P. *Catalysis in Chemistry and Enzymology*; McGraw Hill: New York, 1969.

(3) Jencks, W. P.; Carriuolo, J. General Base Catalysis of the Aminolysis of Phenyl Acetate. *J. Am. Chem. Soc.* **1960**, *82*, 675.

(4) Jencks, W. P.; Gilchrist, M. General Base Catalysis of the Aminolysis of Phenyl Acetate by Primary Alkylamines. *J. Am. Chem. Soc.* **1966**, *88*, 104.

(5) Bruice, T. C.; Donzel, A.; Huffman, R. W.; Butler, A. R. Aminolysis of Phenyl Acetates in Aqueous Solutions. Observations on the Influence of Salts, Amine Structure, and Base Strength. *J. Am. Chem. Soc.* **1967**, *89*, 2106.

(6) Rogers, G. A.; Bruice, T. C. Isolation of a tetrahedral intermediate in an acetyl transfer reaction. *J. Am. Chem. Soc.* **1973**, *95*, 4452.

(7) Rogers, G. A.; Bruice, T. C. Synthesis and evaluation of a model for the so-called charge-relay system of the serine esterases. *J. Am. Chem. Soc.* **1974**, *96*, 2473.

(8) Bruice, T. C.; Benkovic, S. J. Acyl Transfer Reactions Involving Carboxylic Acid Esters and Amides. *Bioorganic Mechanisms*, *Vol. 1*; W. A. Benjamin, Inc.: New York, 1966; Chapter 1.

(9) Bunnett, J. F.; Davis, G. T. The Mechanism of Aminolysis of Esters. *J. Am. Chem. Soc.* **1960**, *82*, 665.

(10) Gresser, M. J.; Jencks, W. P. Ester aminolysis. Structure-reactivity relationships and the rate-determining step in the aminolysis of substituted diphenyl carbonates. *J. Am. Chem. Soc.* **1977**, *99*, 6963.

(11) Williams, A. Concerted mechanisms of acyl group transfer reactions in solution. *Acc. Chem. Res.* **1989**, *22*, 387.

(12) Zipse, H.; Wang, L.; Houk, K. N. Polyether catalysis of ester aminolysis-A computational and experimental study. *Liebigs Ann.* **1996**, *10*, 1511.

(13) Wang, L.; Zipse, H. Bifunctional catalysis of ester aminolysis-A computational and experimental study. *Liebigs Ann.* **1996**, *10*, 1501.

(14) Yang, W.; Drueckhammer, D. G. Computational Studies of the Aminolysis of Oxoesters and Thioesters in Aqueous Solution. *Org. Lett.* **2000**, *2*, 4133.

(15) Oie, T.; Loew, G. H.; Burt, S. K.; Binkley, J. S.; McElroy, R. D. Quantum chemical studies of a model for peptide bond formation: formation of formamide and water from ammonia and formic acid. *J. Am. Chem. Soc.* **1982**, *104*, 6169.

(16) Gorb, L.; Asensio, A.; Tuñón, I.; Ruiz-López, M. F. The Mechanism of Formamide Hydrolysis in Water from *Ab Initio* Calculations and Simulations. *Chem. Eur. J.* **2005**, *11*, 6743.

(17) Chalmet, S.; Harb, W.; Ruiz-Lopez, M. F. Computer Simulation of Amide Bond Formation in Aqueous Solution. *J. Phys. Chem. A* **2001**, *105*, 11574.

(18) Ilieva, S.; Galabov, B.; Schaefer, H. F. Computational Study of the Aminolysis of Esters. The Reaction of Methylformate with Ammonia. *J. Org. Chem.* **2003**, *68*, 1496.

(19) Singleton, D. A.; Merrigan, S. R. Resolution of Conflicting Mechanistic Observations in Ester Aminolysis. A Warning on the Qualitative Prediction of Isotope Effects for Reactive Intermediates. *J. Am. Chem. Soc.* **2000**, *122*, 11035.

(20) Sung, D. D.; Koo, I. S.; Yang, K.; Lee, I. DFT studies on the structure and stability of zwitterionic tetrahedral intermediate in the aminolysis of esters. *Chem. Phys. Lett.* **2006**, *426*, 280.

(21) Lee, I.; Sung, D. D. Theoretical and physical aspects of stepwise mechanisms in acyl-transfer reactions. *Curr. Org. Chem.* **2004**, *8*, 557.

(22) Gresser, M. J.; Jencks, W. P. Ester aminolysis. Structure-reactivity relationships and the rate-determining step in the aminolysis of substituted diphenyl carbonates. *J. Am. Chem. Soc.* **1977**, *99*, 6963.

(23) Castro, E. A.; Stander, C. L. Nonlinear Broensted-type plot in the pyridinolysis of 2, 4-dinitrophenyl benzoate in aqueous ethanol. *J. Org. Chem.* **1985**, *50*, 3595.

(24) Castro, E. A.; Valdiva, J. L. Linear free-energy relationship in the pyridinolysis of 2, 4-dinitrophenyl p-chlorobenzoate in aqueous ethanol solution. *J. Org. Chem.* **1986**, *51*, 1668.

(25) Castro, E. A.; Steinfort, G. B. Kinetics and mechanism of the pyridinolysis of 2, 4-dinitrophenyl *p*-nitrobenzoate. *J. Chem. Soc., Perkin Trans. 2* **1983**, *2*, 453.

(26) Castro, E. A.; Leandro, L.; Quesieh, N.; Santos, J. G. Kinetics and Mechanisms of the Reactions of 3-Methoxyphenyl, 3-Chlorophenyl, and 4-Cyanophenyl 4-Nitrophenyl Thionocarbonates with Alicyclic Amines. *J. Org. Chem.* **2001**, *66*, 6130.

(27) Castro, E. A.; Galvez, A.; Leandro, L.; Santos, J. G. Kinetic and Mechanistic Investigation of the Aminolysis of 3-Methoxyphenyl 3-Nitrophenyl Thionocarbonate, 3-Chlorophenyl 3-Nitrophenyl Thionocarbonate, and Bis (3-nitrophenyl) Thionocarbonate. *J. Org. Chem.* **2002**, *67*, 4309.

(28) Um, I. H.; Lee, S. E.; Kwon, H. J. Effect of Amine Nature on Reaction Mechanism: Aminolyses of *O*-4-Nitrophenyl Thionobenzoate with Primary and Secondary Amines. *J. Org. Chem.* **2002**, *67*, 8999.

(29) Oh, H. K.; Kim, S. K.; Cho, I. H.; Lee, H. W.; Lee, I. Kinetics and mechanism of the aminolysis of aryl phenyldithioacetates in acetonitrile. *J. Chem. Soc., Perkin Trans. 2* **2000**, *2*, 2306.

(30) Antonczak, S.; Ruiz-Lopez, M. F.; Rivail, J. L. Ab Initio Analysis of Water-Assisted Reaction Mechanisms in Amide Hydrolysis. *J. Am. Chem. Soc.* **1994**, *116*, 3912.

(31) Díaz, N.; Suárez, D.; Sordo, T. L.; Merz, K. M., Jr. A Theoretical Study of the Aminolysis Reaction of Lysine 199 of Human Serum Albumin with Benzylpenicillin: Consequences for Immunochemistry of Penicillins. *J. Am. Chem. Soc.* **2001**, *123*, 7574.

(32) Díaz, N.; Suárez, D.; Sordo, T. L. Theoretical Study of the Water-Assisted Aminolysis of *â*-Lactams: Implications for the Reaction between Human Serum Albumin and Penicillins. *J. Am. Chem. Soc.* **2000**, *122*, 6710.

(33) Díaz, N.; Suárez, D.; Sordo, T. L. Importance of a Synperiplanar Stepwise Mechanism through Neutral Intermediates in the Aminolysis of Monocyclic *â*-Lactams: A Theoretical Analysis. *J. Org. Chem.* **1999**, *64*, 9144.

(34) Díaz, N.; Suárez, D.; Sordo, T. L. NH_3-Assisted Ammonolysis of *â*-Lactams: A Theoretical Study. *J. Org. Chem.* **1999**, *64*, 3281.

(35) Díaz, N.; Suárez, D.; Sordo, T. L. Ammonolysis and Aminolysis of b-Lactams: A Theoretical Study. *Chem. Eur. J.* **1999**, *5*, 1045.

(36) Díaz, N.; Suárez, D.; Sordo, T. L.; Me'ndez, R.; Villacorta, J. M. A Combined Theoretical and Experimental Research Project into the Aminolysis of β-Lactam Antibiotics: The Importance of Bifunctional Catalysis. *Eur. J. Org. Chem.* **2003**, 4161.

(37) Díaz, N.; Suárez, D.; Sordo, T. L. Theoretical Study of Amine-Assisted Aminolysis of Penicillins - The Kinetic Role of the Carboxylate Group. *Eur. J. Org. Chem.* **2001**, 793.

(38) Díaz, N.; Suárez, D.; Sordo, T. L. Theoretical Study of Ammonolysis of Monobactams: Kinetic Role of the N-Sulfonate Group. *Helv. Chim. Acta* **2002**, *85*, 206.

(39) Ilieva, S.; Galabov, B.; Musaev, D. G.; Morokuma, K. Computational Study of the Aminolysis of 2-Benzoxazolinone. *J. Org. Chem.* **2003**, *68*, 3406.

(40) Jin, L.; Wu, Y.; Xue, Y.; Guo, Y.; Xie, D. Q.; Yan, G. S. Theoretical Studies on the Aminolysis of Phenyl Formate. Mechanism and Solvent Effect. *Acta Chim. Sin.* **2006**, *64*, 873.

(41) Yi, G. Q.; Zeng, Y.; Xia, X. F.; Xue, Y.; Kim, C. K.; Yan, G. S. The substituent effects of the leaving groups on the aminolysis of phenyl acetates: DFT studies. *Chem. Phys.* **2008**, *345*, 73.

(42) Xue, Y.; Kim, C. K. Effects of Substituents and Solvents on the Reactions of Iminophosphorane with Formaldehyde: *Ab Initio* MO Calculation and Monte Carlo Simulation. *J. Phys. Chem. A* **2003**, *107*, 7945.

(43) Xue, Y.; Kim, C. K.; Guo, Y.; Xie, D. Q.; Yan, G. S. DFT study and Monte Carlo simulation on proton transfers of 2-amino-2-oxazoline, 2-amino-2-thiazoline, and 2-amino-2-imidazoline in the gas phase and in water. *J. Comput. Chem.* **2005**, *26*, 994.

(44) Wu, Y.; Xue, Y.; Xie, D. Q.; Kim, C. K.; Yan, G. S. Theoretical Studies on the Hydrolysis Mechanism of N-(2-oxo-1,2-dihydro-pyrimidinyl) Formamide. *J. Phys. Chem. B* **2007**, *111*, 2357.

(45) Frisch, M. J.; Trucks, G. W.; Schlegel, H. B.; Scuseria, G. E.; Robb, M. A.; Cheeseman, J. R.; Zakrzewski, V. G.; Montgomery, J. A., Jr.; Stratmann, R. E.; Burant, J. C.; Dapprich, S.; Millam, J. M.; Daniels, A. D.; Kudin, K. N.; Strain, M. C.; Farkas, O.; Tomasi, J.; Barone, V.; Cossi, M.; Cammi, R.; Mennucci, B.; Pomelli, C.; Adamo, C.; Clifford, S.; Ochterski, J.; Petersson, G. A.; Ayala, P. Y.; Cui, Q.; Morokuma, K.; Malick, D. K.; Rabuck, A. D.; Raghavachari, K.; Foresman, J. B.; Cioslowski, J.; Ortiz, J. V.; Stefanov, B. B.; Liu, G.; Liashenko, A.; Piskorz, P.; Komaromi, I.; Gomperts, R.; Martin, R. L.; Fox, D. J.; Keith, T.; Al-Laham, M. A.; Peng, C. Y.; Nanayakkara, A.; Gonzalez, C.; Challacombe, M.; Gill, P. M. W.; Johnson, B.; Chen, W.; Wong, M. W.; Andres, J. L.; Gonzalez, C.; Head-Gordon, M.; Replogle, E. S.; Pople, J. A. *Gaussian 03, Revision D. 01*; Gaussian, Inc.: Pittsburgh, PA, 2005.

(46) Fukui, K. Formulation of the reaction coordinate. *J. Phys. Chem.* **1970**, *74*, 4161.

(47) Reed, A. E.; Curtiss, L. A.; Weinhold, F. Intermolecular interactions from a natural bond orbital, donor-acceptor viewpoint. *Chem. Rev.* **1988**, *88*, 899.

(48) Jorgensen, W. L.; Ravimohan, C. Monte Carlo simulation of differences in free energies of hydration. *J. Chem. Phys.* **1985**, *83*, 3050.

(49) Jorgensen, W. L.; Tirado-Rives, J. *J. Comput. Chem.* **2005**, *26*, 1689–1700.

(50) Marcus, R. A. On the Theory of Oxidation-Reduction Reactions Involving Electron Transfer. *J. Chem. Phys.* **1956**, *24*, 966.

(51) Yoo, H. Y.; Houk, K. N. Theory of Substituent Effects on Pericyclic Reaction Rates: Alkoxy Substituents in the Claisen Rearrangement. *J. Am. Chem. Soc.* **1997**, *119*, 2877.

(52) Murdoch, J. R. Relationship between More O'Ferrall plots and Marcus rate theory. Overriding orbital-symmetry constraints on chemical reactions. *J. Am. Chem. Soc.* **1983**, *105*, 2660.

(53) Murdoch, J. R. A simple relationship between empirical theories for predicting barrier heights of electron-, proton-, atom-, and group-transfer reactions. *J. Am. Chem. Soc.* **1983**, *105*, 2159.

CT800099A